Check for updates

Water Science & Technology

IWA PUBLISHING

© 2022 The Authors

Water Science & Technology Vol 85 No 4, 970 doi: 10.2166/wst.2022.031

Physical characterization and kinetic studies of Zn (II) biosorption by *Morganella morganii* ACZ05

D. Ramya [c,*], A. Joseph Thatheyus[a], S. Jemima Balaselvi Juliana [b], N. Jennifer Michellin Kiruba [c] and Deborah Gnana Selvam A[c]

[a] Postgraduate & Research Department of Zoology, The American College, Madurai 625 002, Tamil Nadu, India
[b] Postgraduate & Research Department of Chemistry, The American College, Madurai 625 002, Tamil Nadu, India
[c] Department of Microbiology, The American College, Madurai 625 002, Tamil Nadu, India
*Corresponding author. E-mail: ramya.susila@gmail.com

DR, 0000-0003-1653-0826; SJBJ, 0000-0003-0610-0371; NJMK, 0000-0002-9595-7096

ABSTRACT

Through this investigation, we establish the mechanism and physical characterization of zinc (II) sequestration by *Morganella morganii* ACZ05 strain, which was isolated and characterized from soil polluted by effluents from electroplating industries. As far as we know, there is very little literature concerning zinc biosorption using an environmental strain of *M. morganii*. The SEM analysis shows the dark porous gaps in the aggregated cell-matrix of test bacterial biomass which is inferred as water channels usually seen in biofilms, as compared to metal-unexposed control. *M. morganii* is not known to produce biofilms unless in the rare nosocomial conditions. Here, SEM analysis shows the production of biofilms after exposure to zinc (II) at 500 ppm, which has not been previously reported. EDX analysis of bacterial biomass also specified the sorption of zinc (II) by the bacterial cells and the presence of new peaks for zinc in contrast to control. Both XRD and FTIR analysis observations strongly implicate the potential of physical adsorption as a mechanism for heavy metal resistance. Analysis of the cell surface by Atomic force microscopy and examination of the topography revealed cell aggregation occurs during biofilm production after zinc biosorption. Unlike other reports, regular models such as Langmuir isotherm and Freundlich isotherm were found insufficient to explain the physisorption of zinc (II) metal ions on complex multicomponent adsorbents such as the exopolymeric surface of the bacterial cells. However, adsorption kinetics of zinc (II) to the bacterial biomass was most effectively elucidated by a pseudo-second-order kinetic model, suggesting a certain kind of chemisorption that requires further study.

Key words: Biosorption, Freundlich, Langmuir, *M. morganii* ACZ05, SEM/EDX, zinc II)

HIGHLIGHTS

- XRD and FTIR – potential of physical adsorption as a mechanism for heavy metal resistance.
- SEM-EDX and AFM – morphological changes were observed after metal addition.
- The isotherm studies – fit of pseudo-second order for biosorption experimental data suggests the involvement of cellular mechanisms for the activity of binding sites of metal ions and other chemical sorption processes.
- Biosorption, chemisorption,

This is an Open Access article distributed under the terms of the Creative Commons Attribution Licence (CC BY 4.0), which permits copying, adaptation and redistribution, provided the original work is properly cited (http://creativecommons.org/licenses/by/4.0/).

Downloaded from http://iwaponline.com/wst/article-pdf/85/4/970/1016325/wst085040970.pdf
by guest

GRAPHICAL ABSTRACT

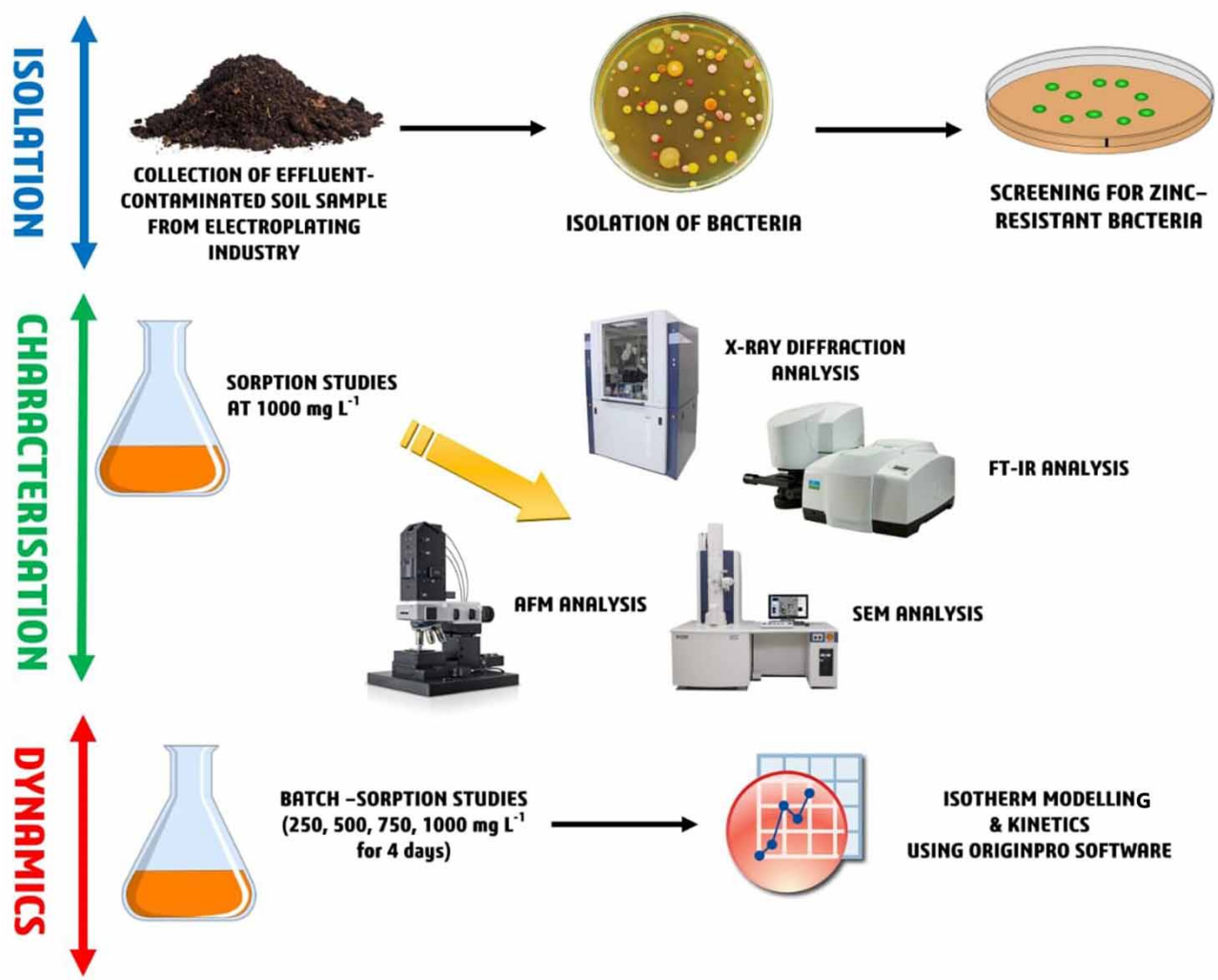

1. INTRODUCTION

The need for an effective mechanism of biosorption is called for by the widespread nature of metal toxicity and pollution in different types of water resources. Adsorption of contaminant metal ions by dead or live biomass of microorganisms such as fungi and bacteria, is often referred to as microbial biosorption (Fomina & Gadd 2014). Metabolic by-products of microorganisms include proteins, polysaccharides, enzymes, and extracellular polymeric substances (EPS), which often possess metal-binding properties (Gadd 2009). To understand the binding mechanism of metal and bacteria, a study of the chemical nature of the biomass is undertaken (Kumar *et al.* 2010). Studies reveal that the polysaccharide component of microbial cell walls has several chemical groups that provide binding sites for metal ions. These substances contribute to the chelation of contaminating heavy metal ions, eliminating them from the source (Ahluwalia & Goyal 2007; Wang & Chen 2009). XRD and FTIR analysis of the bacterial biomass can give insight into the different functional groups involved in metal biosorption, whereas AFM and SEM–EDX shows the change in the morphology of the cell surface upon metal exposure (Ahalya *et al.* 2003; Park *et al.* 2010). When these procedures are taken together, they provide an overall idea of the biosorption mechanism involved (Park *et al.* 2010).

The mechanism of sorption is not often possible to determine quantitatively. The multiple metabolic processes of a bacterial or fungal cell can also heavily impact the nature of the sorption mechanism. Therefore, biosorption can often fail to adhere to the numerous adsorption isotherm models developed about metal sorption. But they can provide an insight into the

Downloaded from http://iwaponline.com/wst/article-pdf/85/4/970/1016325/wst085040970.pdf
by guest

involvement of various modes of sorption such as physisorption and chemisorption of metal ions on the surface of the biosorbent (Kotrba 2011).

Similar studies indicate that heavy metal biosorption can be modeled using Langmuir and Freundlich isotherm models. These models are uncomplicated, dependent on two parameters, concentration and time, which points us towards the equilibrium reached under experimental conditions. The Langmuir model stipulates that the surface of the bacterial biomass has different binding sites that possess affinity towards certain metal ions but the adsorbate molecules do not interact with each other, probably creating a monolayer. On the contrary, the Freundlich isotherm model supposes that occupancy of adjacent sites for the binding of metals and the bond energy between the adsorbent and adsorbate are related (Lu *et al.* 2006; Gabr *et al.* 2008; Joo *et al.* 2010; Huang & Liu 2013).

The sorbate and the biosorbent are pushed forward in an adsorption reaction to reach equilibrium, in an aqueous phase, which determines the sorbent's maximum uptake ability. The kinetics data of the sorption provides us optimum levels of all parameters such as sorbate removal efficiencies, adsorbent (biomass) concentrations, pH, and temperature. These contribute significantly during the development of a wastewater treatment plant or a setup (Derco & Vrana 2018). During sorption studied in batch reactor conditions, kinetic data are characterized by verifiable models that is, pseudo-first and -second-order models (Kotrba 2011).

The metal ion and biosorbent surface interact in two phases due to their biphasic nature. 90% of the biosorption occurs in the initial phase, which is rapid and plateaus for a fixed time. The second phase of biosorption occurs rather more slowly, lasting up to 4 hours. For example, in a study by Çeribasi & Yetis (2001), when *Phanerochaete chrysosporium* is exposed to varying concentrations of nickel and lead, maximum adsorption was attained usually in the first 30 minutes, whereas it took 3 hours to reach equilibrium. Lu *et al.* (2006) reported the biosorption kinetics and equilibria of lead (Pb), cadmium (Cd) and copper (Cu) ions by *Enterobacter* sp. The results showed that the biomass of *Enterobacter* sp. was an efficient adsorbent of lead (Pb), cadmium (Cd) and copper (Cu) ions suggesting good recyclable nature of the biosorbent. For analysis, kinetics of heavy-metal adsorption by *Enterobacter* sp. and the model seemed to have an outstanding prediction of the experimental information. Likewise, *Morganella* showed better metal removal efficiency. *Morganella* is a type of Gram-negative microbe belonging to the family Enterobacteriaceae, members of which were formerly planned as a candidate in bioremediation of chromium (VI), Lead (II) and uranium (VI) (Martins *et al.* 2010; Kumar *et al.* 2020; Princy *et al.* 2020).

Our study determined the biosorption of Zn (II) by *M. morganii* ACZ05. Equilibrium dynamics and kinetics of the biosorption were investigated under batch reactor conditions by atomic absorption spectroscopy. Isotherm modeling and kinetics models were fitted with experimental data to determine the best fit. XRD, FT-IR, SEM-EDX, and AFM were used to examine the changes in the biosorbent surface post-sorption, and mode of biosorption.

2. MATERIALS AND METHODS

2.1. Media used and growth conditions

A single Zn (II) resistant bacterial strain, *M. morganii* ACZ05, was characterized from soil near electroplating industries situated in the Jaihindpuram area of Madurai. 100 µl of the soil and effluent samples were plated onto sterile nutrient agar plates after diluting them to 10^{-6}. The nutrient agar media contained: Peptone (5 g/l), sodium chloride (5 g/l), HM peptone B (1.5 g/ml), yeast extract (1.5 g/l), agar (15 g/l) at 28 °C. The pH of the growth medium was adjusted to 7.2 by the addition of 1 M KOH prior to autoclaving. The bacterial isolates were then grown for 24 hrs at 37 °C. A total of ten zinc metal-resistant bacterial strains were isolated. Among the ten strains, two strains were able to tolerate 1,000 ppm concentration of zinc (II) metal. From these, the highest tolerant bacterial strain was chosen for the study.

The bacterial isolates so obtained, were tested for tolerance in different concentrations (250 mg L^{-1}, 500 mg L^{-1}, 750 mg L^{-1} and 1,000 mg L^{-1}) of zinc (II). After incubation at 37 °C for 24 h, the bacterial strain which could tolerate 1,000 mg L^{-1} zinc was selected and identified as *M. morganii* ACZ05 (GenBank Accession No: KJ830754).

2.2. Preparation of metal stock solutions

Zinc sulfate ($ZnSO_4.7H_2O$) was dissolved in double distilled water to get a standard solution of zinc (II) (1,000 mg L^{-1}). Atomic absorption spectrophotometer (ELICO Technologies Pvt. Ltd, India) was used to measure the zinc (II) metal ion concentration in all samples.

Downloaded from http://iwaponline.com/wst/article-pdf/85/4/970/1016325/wst085040970.pdf
by guest

2.3. Bioremoval of zinc (II) using the bacterial strain *M. morganii* ACZ05

One ml of overnight culture was inoculated into 500 ml Erlenmeyer flasks with 300 ml nutrient broth spiked with zinc (II) (250, 500, 750, and 1,000 mg L^{-1}) and incubated for four days and later optimized to 1–15 minutes. From this, a clear supernatant was obtained by centrifuging an aliquot (10 ml) of the sample at 2,500 rpm. The clear supernatant was subjected to acid digestion, and the residual concentration of zinc (II) ions were measured.

2.4. XRD analysis

The diffraction pattern of the biomass powder samples of untreated control and test samples were analyzed using XRD-6000. The diffracted X-ray intensities were recorded using a copper anode, with a step size of 0.0500, in a range of 10–80°, with an XPERT-PRO diffractometer system.

2.5. FTIR analysis

The bacterial cells were harvested before and after the adsorption of Zn (II) ions. The bacterial biomass was centrifuged for ten minutes at 3,000 rpm and washed repeatedly with 0.9% saline solution at a pH 6.5 (Deokar *et al.* 2013). Then, they were prepared by the potassium bromide (KBr) method and their profiles were observed (4,000–400 cm^{-1}) on an FTIR spectrometer (Bruker, alpha).

2.6. Scanning electron microscopy (SEM) of *M. morganii* ACZ05 without metal (control) and *M. morganii* ACZ05 treated with zinc (II)

SEM images were taken to make ultrastructural observations of bacterial cells (Srivastava & Thakur 2007) using Field-Emission Scanning Electron Microscope [Carl Zeiss ultra 55; 5 kV with X-ray spectroscopy (EDX)]. The bacterial biomass was harvested, centrifuged, and fixed by glutaraldehyde (2.5%) following dehydration using ethanol. The mounts were dried using tetramethylsilane and coated with gold before documentation.

2.7. Atomic force microscopy of *M. morganii* ACZ05 without metal (control) and *M. morganii* ACZ05 treated with zinc (II)

The bacterial biomass, harvested following centrifugation and smeared on glass slides, before being dried at a temperature of 22–28 °C. SPM 100 Atomic force microscope was used to view and document the samples.

2.8. Sorption equilibrium studies

One ml of an overnight culture of *M. morganii* ACZ05 was inoculated into 300 ml nutrient broth spiked with zinc (II) at concentrations of 250, 500, 750, and 1,000 mg L^{-1}, and incubated. 10 ml of the sample was centrifuged at 2,500 rpm every 24 hours for 4 days. The clear supernatant was subjected to acid digestion and used for AAS analysis (Devika *et al.* 2014).

AAS Data evaluation for Zn(II) sorption:

In the batch sorption studies carried out for the biosorption of Zn(II) ions by *Morganella morganii* ACZ05 bacterial biomass, the maximum amount of metal ion adsorbed by the bacterial biomass is calculated as follows (Hussein *et al.* 2004).

Considering the equilibrium,

$$Morganella\ morganii\ \text{ACZ05} + Zn(II)_{initial} \rightleftharpoons\ Morganella\ morganii\ \text{ACZ05}: Zn(II) + Zn(II)_{final}$$

where $Zn(II)_{initial} = 250$, 500, 750, and 1,000 mg L^{-1} batches, formulated as C_i and $Zn(II)_{final}$ are free unsorbed metal ions determined every 24 hours for four days in each of the above batches. The value of $Zn(II)_{final}$ is determined from AAS and formulated as C_e in the following equation.

$$Q_e = (C_i - C_e) \times \frac{V}{m}$$

where Q_e is the amount of Zn(II)(mg) adsorbed by per gram of *M. morganii* ACZ05 (mg/g),

V is the volume of bulk liquid sample (ml),

C_i is the initial concentration of the Zn (II) in the solution (mg/L),

Downloaded from http://iwaponline.com/wst/article-pdf/85/4/970/1016325/wst085040970.pdf
by guest

C_e is the final concentration of the Zn(II) in the solution at equilibrium (mg/L)

and m is the amount of the *M. morganii* ACZ05 added to bulk liquid (mg).

The obtained results are analyzed using the Langmuir adsorption isotherm and the Freundlich isotherm models.

The Langmuir adsorption model is given by:

$$Q_e = \frac{Q_{max} b C_e}{1 + bC_e}$$

where Q_{max} is the maximum amount of metal adsorbed under the experimental conditions employed, b is a constant that represents the strength of the adsorption between the biosorbent and sorbate.

The linearized form of the Langmuir model states is given by $C_e/q_e = 1/bQ_{max} + C_e/Q_{max}$. A plot of C_e/q_e vs C_e will be linear with a slope $1/Q_{max}$ and y-intercept $1/bQ_{max}$.

R_L is the dimensionless separation factor that is considered in the Langmuir model. It determines the capacity of adsorption between the biosorbate and the biosorbent in the two different phases, such as solid and liquid. (Horsfall Jnr & Spiff 2005). It is given by the expression, $R_L = 1/1 + bC_O$ where b is the Langmuir constant (mg/L) and C_0 is an initial concentration of biosorbate (metal ions) in the solution (mg/L).

The factor R_L determines the direction and feasibility of the reaction between the metal ion and biosorbent, as the isotherm to be either unfavorable ($R_L > 1$), linear ($R_L = 1$), favorable ($0 < R_L < 1$), or irreversible ($R_L = 0$).

The Freundlich adsorption model is given by $q_e = kC_e^{1/n}$, where k and n are Freundlich constants, which correlate to the maximum adsorption capacity and adsorption intensity, respectively. The linearized form of the Freundlich equation is given by $lnq_e = lnk + 1/nlnC_e$; Sips (1948) proposed an empirical isotherm equation, also identified as the Langmuir–Freundlich isotherm, which is often expressed as:

$$q_e = \frac{K_S Ce^{ns}}{1 + a_S Ce^{ns}}$$

where K_S is the Sips constant (mg/L), a_S is the affinity coefficient (mg/L) and ns is the heterogeneity coefficient.

2.9. Kinetic studies

Kinetic experiments were conducted by mixing 10 mg biosorbent of *M. morganii* ACZ05 with series of 100 ml nutrient broth containing 500 mg L^{-1} of zinc(II) and incubated at 30 °C and optimum pH 6. Samples were drawn at 1, 3, 5,10- and 15-minute intervals. A mixing speed of 200 rpm was used for this set of experiments. After centrifugation, the supernatant subjected to acid digestion was examined for remaining metal ions concentration (Oh *et al.* 2009). Lagergren's pseudo-first-order and pseudo-second-order equations were used to model the kinetics of heavy metals.

3. RESULTS

3.1. X-ray diffraction (XRD) studies

Figure 1(a) demonstrates the sorption of zinc (II) on *M. morganii* ACZ05 and the untreated control. The XRD profile of the control shows a lack of any separate characteristic peak. The XRD examination showed that the zinc (II) loaded *M. morganii* ACZ05 cells had five characteristic diffraction peaks at $2\theta = 21.39°$, 25.45°, 36.36°, 26.20°, and 31.60°, equivalent to the hkl values of 111, 040, 220, 002, and 044 surfaces of crystalline zinc particles. Comparison of corresponding *d*-spacing values of 4.15, 3.49, 2.53, 3.39, and 2.82 with data files of standard compounds (JCPDS) exhibited a suitable relationship with the lines of zinc oxide sulfate, zinc sulfate, and sulfur compounds.

3.2. Fourier transform infrared (FTIR) studies

FTIR analysis of zinc (II) biosorption by *M. morganii* ACZ05 showed a change in frequency from 3,417.09 to 3,314.04. Figure 1(b) depicts the FTIR spectra of control and zinc-loaded *M. morganii* ACZ05. The adsorption band shifted from 1,083.14 to 1,079.58.

Downloaded from http://iwaponline.com/wst/article-pdf/85/4/970/1016325/wst085040970.pdf
by guest

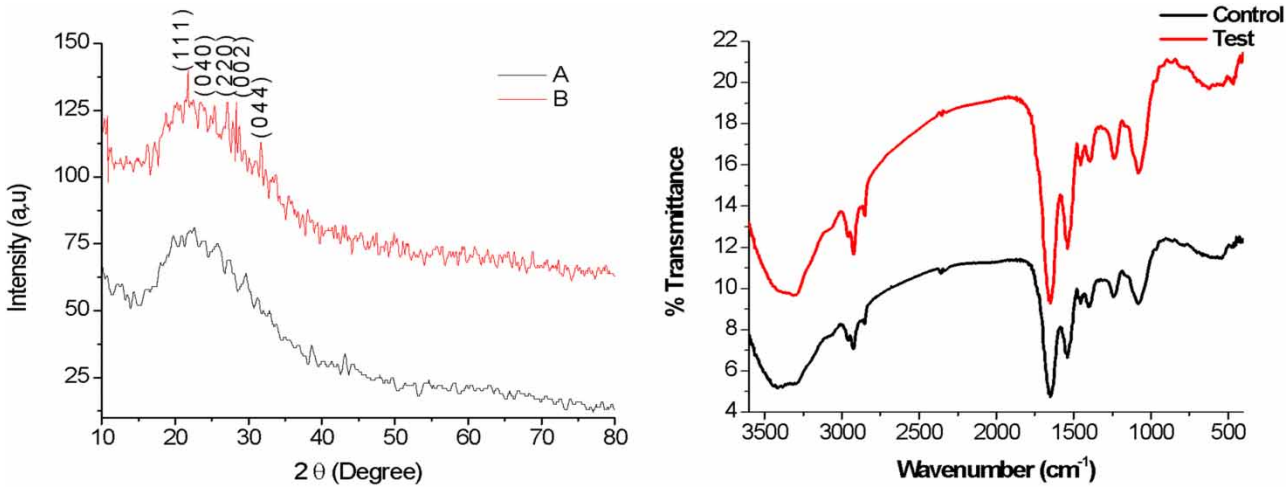

Figure 1 | (a) XRD analysis of zinc (II) biosorption by *M. Morganii* ACZ05 and (b) FTIR analysis of zinc (II) biosorption by *M. Morganii* ACZ05.

3.3. Scanning electron microscopy (SEM) and energy dispersive X-ray (EDX) studies

SEM and EDX studies were employed to check for the presence and the characterization of metal ions adsorbed to the biomass. Before zinc (II) adsorption, the structure of the bacterial biomass appeared as long, thin, rods. Following the adsorption of zinc, a considerable change in the morphology was detected (Figure 3). The morphological changes of the bacterial cells, which looked fat, spongy, and plumped, could be accredited to the treatment of the cell surface with zinc ions. This observation is in agreement with the elemental analysis of cells.

The biomass' energy dispersive spectrum after zinc (II) uptake is revealed in Figure 2. It indicated the presence of separate peaks for zinc, potassium, calcium but no peak for sodium and silicon. The atomic percentage of Zn (at%) was 0.27, while that of Al decreased, from 3.27 to 1.95, while that of C, Mg, P, S, and Cl increased from 30.20 to 30.40, 0.03 to 0.09, 0.15 to 0.59, 0.04 to 0.21 and 0.04 to 0.13 after zinc uptake. The observations indicated that zinc can form covalent bonds with C-, O- and P- containing functional groups during adsorption.

3.4. Atomic force microscopy (AFM) studies

AFM was employed to study the cell topological characterization of *M. morganii* ACZ05 biomass before and subsequently after zinc (II) adsorption (Figure 3). Observation from the Atomic force microscopic study depicted the collection of zinc precipitates on the external surface of the bacteria. The surface irregularity of bacteria was increased when the bacteria interacted with zinc. The control biomass without zinc exposure had smooth surfaces. Following the sorption of zinc, the cell's morphology was altered into a spindle-like structure.

3.5. Adsorption isotherms

The sorption capacity of *M. morganii* ACZ05 for Zn (II) was determined by fitting experimental data into the commonly used linearized Langmuir isotherm and Freundlich isotherm models.

Application of isotherm models to describe the adsorption of Zn (II) ions by *M. morganii* ACZ05 with a treatment period of four days was quite unsuccessful, largely due to the low fit of the experimental data on linearization. The Langmuir constant Q_{max} and b values were higher in the second and fourth days. Though the correlation coefficient for the Langmuir isotherm model was the maximum on day one of adsorption (R^2 value 0.33) the values were far below the threshold of $R^2 > 0.9$ (Figure 4(a)–4(d)). But the Freundlich isotherm model was the maximum on day one of adsorption 0.99. The R_L value of Zn (II) adsorptions was near 1 for all four days of the treatment period but only day one registered a lower R_L value of 0.56. The Freundlich constant n was high on the fourth day ($n = 4.02$) and it decreased continuously for the third ($n = 1.24$), second ($n = 0.84$) and first day ($n = 0.12$) of the treatment period. From the table above, based on the R^2 values it is quite easily visible that Langmuir, Freundlich and Sips isotherms are not a good fit for the experimental data on all four days (Table 1).

Downloaded from http://iwaponline.com/wst/article-pdf/85/4/970/1016325/wst085040970.pdf
by guest

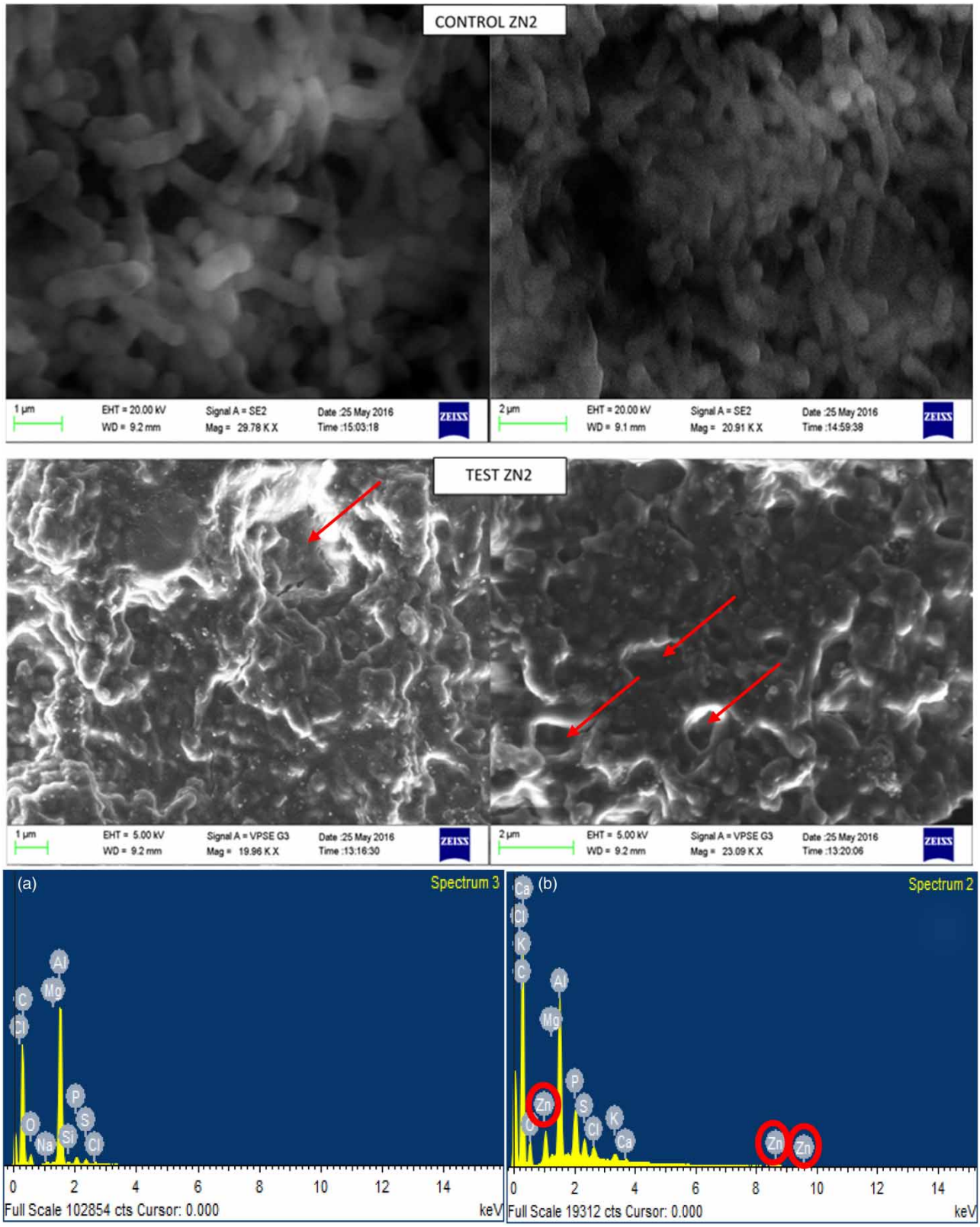

Figure 2 | (I) SEM analysis of biosorption of zinc by *M. morganii* ACZ05. (II) Energy dispersive X-ray analyses of *M. morganii* ACZ05 biomass: (a) before and (b) after zinc (II) accumulation.

Downloaded from http://iwaponline.com/wst/article-pdf/85/4/970/1016325/wst085040970.pdf
by guest

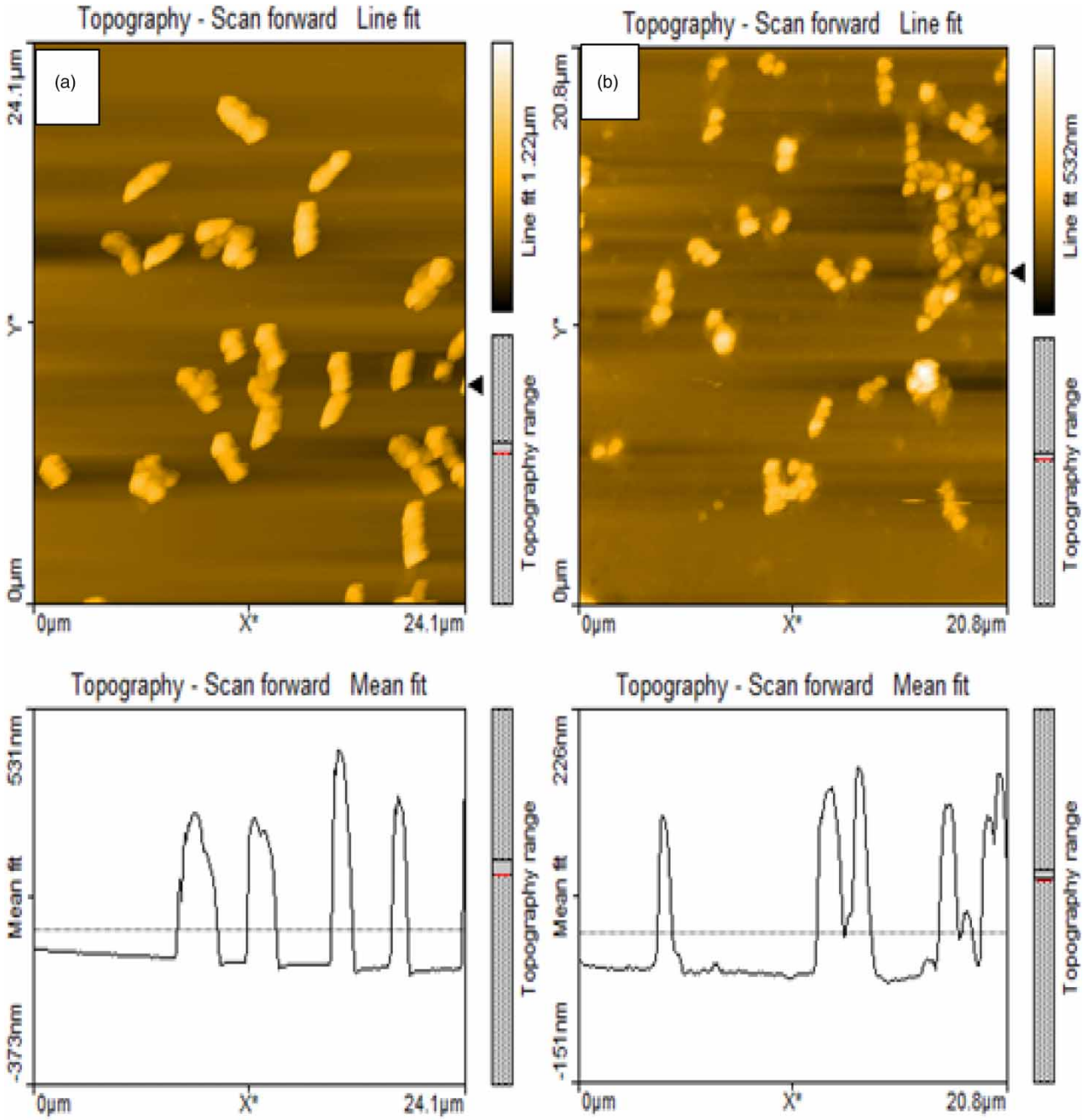

Figure 3 | Atomic Force micrograph of biosorption of zinc by *M. morganii* ACZ05 (a) before zinc exposure (b) after zinc exposure.

3.6. Kinetic studies

The kinetics of biosorption of Zn (II) ions by *M. morganii* ACZ05, the pseudo-second-order was a perfect fit for the experimental data at the correlation coefficient $R^2 = 1$, and the equilibrium constant K_2 was 0.0002. While the correlation coefficient derived using Lagregen's equation (pseudo-first-order) was low and insignificant at $R^2 = 0.57$ and the equilibrium constant K_1 was 0.0007 is shown in Table 2 and Figure 5.

4. DISCUSSION

When *M. morganii* ACZ05 was analyzed for its metal removal capacity under varying concentrations of Zn(II) ions, the optimum concentration was detected to be about 500 mg L^{-1}.

Downloaded from http://iwaponline.com/wst/article-pdf/85/4/970/1016325/wst085040970.pdf
by guest

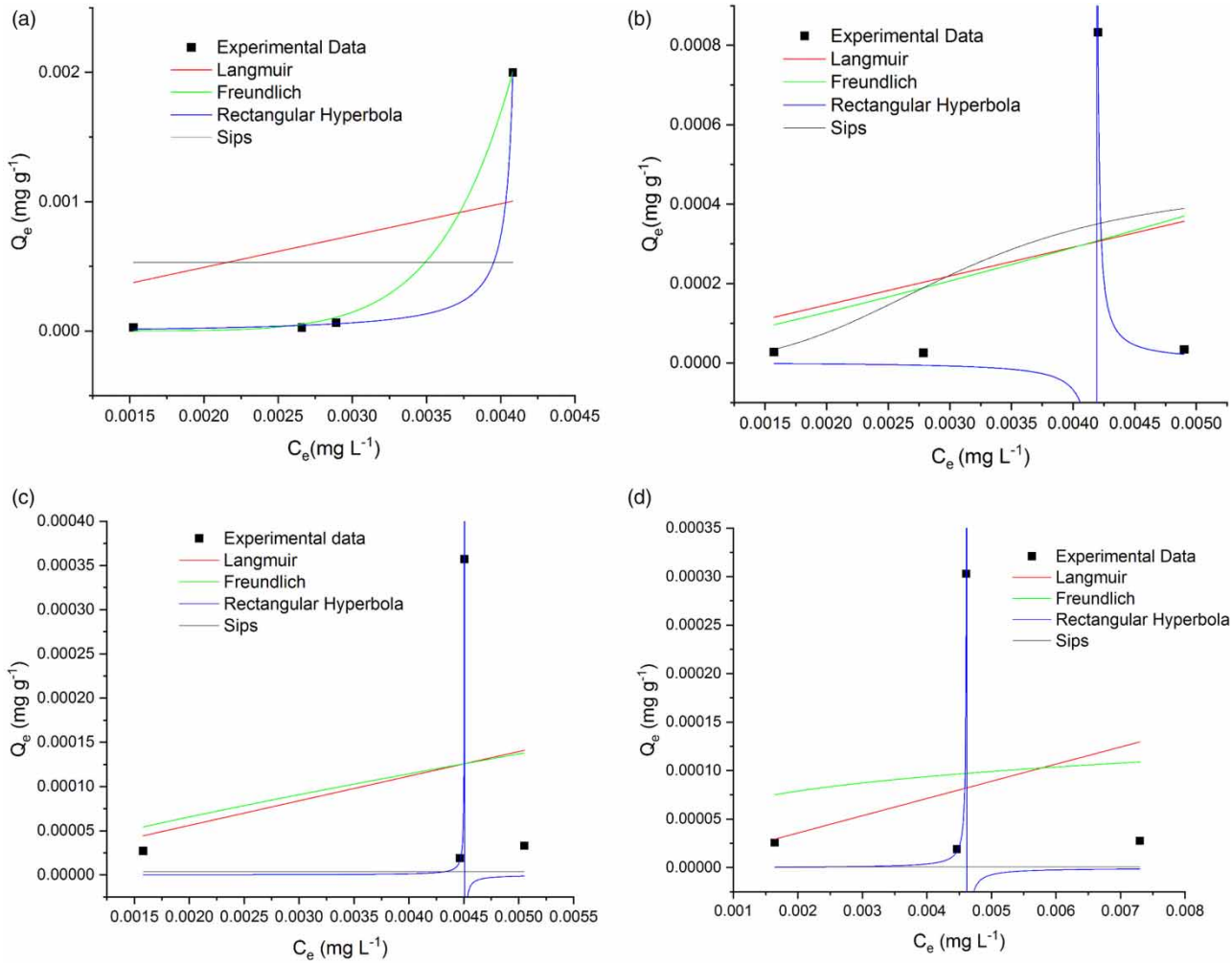

Figure 4 | (a) Isotherm models for Zinc (II) biosorption by the biomass of *M. morganii* ACZ05 for Day 1 of treatment period. (b) Isotherm models for Zinc (II) biosorption by the biomass of *M. morganii* ACZ05 for Day 2 of treatment period. (c) Isotherm models for zinc (II) biosorption by the biomass of *M. morganii* ACZ05 for Day 3 of treatment period. (d) Isotherm models for zinc (II) biosorption by the biomass of *M. morganii* ACZ05 for Day 4 of treatment period.

X-ray scattering profiles of both the control and test display broad characteristic peaks with weak diffraction patterns. On the other hand, according to Shimazu *et al.* (2000), sharp and narrow characteristic peaks and diffraction patterns are analogous to the crystalline nature of the sample. This could be ascribed to the polymeric nature of the bacterial biomass. While the bacterial biomass contains cell wall components such as lipopolysaccharides, surface protein, and other biomolecules, it is presumed that the test sample contains extracellular polysaccharides. Heavy metal resistant strains of bacteria are often found to produce extracellular polymeric substances encased within biofilm that protect the cells from metal toxicity and stress (Teitzel & Persek 2003). Both cell membrane biomolecules and exopolysaccharides are materials that are highly polymeric, largely amorphous, and carbonaceous in structure. Since amorphous samples often generate large amounts of background noise in the form of broad peaks, the nature of the X-ray scattering profile is often difficult to interpret. Chemical and structural changes in crystalline compounds are often studied and interpreted together via FTIR along with XRD. Therefore, further studies on the mechanism of biosorption by *M. morganii* ACZ05 included analysis using FTIR, followed by microscopic techniques.

FTIR analysis was used to check the nature of functional/chemical groups responsible for the biosorption of heavy metals. The characters of the binding sites and their participation in biosorption can be roughly assessed with FTIR. Pagnanelli *et al.* (2000) reported that the control biomass recorded a spectrum between the 3,500 and 3,200 cm^{-1} region caused by the stretching of the N-H bond in the amino groups. They also reported that the peak similar to the above studies, which is observed

Downloaded from http://iwaponline.com/wst/article-pdf/85/4/970/1016325/wst085040970.pdf
by guest

Table 1 | Isotherm model constants for the biosorption of zinc (II) by the biomass of *M. morganii* ACZ05

	Langmuir			Freundlich			Rectangular Hyperbola			Sips			
Days	Q_{max}	b	R^2	K_f	n	R^2	a	b	R^2	K_s	a	b	R^2
1	0.25	2.15E42	0.33	4.44E17	0.12	0.99	−2.4E − 5	−242.1	0.99	−0.83	−1,559.05	−0.19	1.19E − 05
2	1.47	0.052	0.13	0.20	0.84	0.13	3.15E − 6	−238.90	0.99	18,93,428.78	4.19E9	3.82	0.20
3	0.78	0.037	0.07	0.01	1.24	0.07	−1.51E − 7	−221.91	0.97	405.63	1.1E8	−3.75	−0.54
4	31.24	5.73E − 4	−0.08	3.70E − 4	4.02	0.02	−5.69E − 7	−216.59	0.97	42,668.27	8.27E10	−85.97	−0.59

Downloaded from http://iwaponline.com/wst/article-pdf/85/4/970/1016325/wst085040970.pdf
by guest

Table 2 | Pseudo-first and second-order adsorption kinetics of Zn (II) by the biomass of *M. morganii* ACZ05

Metal	R^2	K_1	K_2	R^2
Zn (II)	0.57	0.0007	0.0002	1

between 3,200 and 3,600 cm^{-1} might be caused by the hydroxyl group. Kazy *et al.* (2009) reported that binding of Uranium and Thorium exhibited a strong band at 1,000 and 1,100 cm^{-1} showing that the carboxyl groups are involved in biosorption. Kazy *et al.* (2006) observed varying arrangement and intensity of peak at the region between 800 and 400 cm^{-1} which might be due to the development of strong δ (M–O) and δ (O–M–O) bonds (where M refers to the metal ion).

Minor changes in the peak frequencies between control and test may determine the weakening or strengthening of bond orders in the functional groups involved. A shift in energy frequency of the signature peaks to lower bond orders indicates the weakening of metal-binding sites. Moreover, such interactions of metal ions with the biomass including breaking and formations of new bonds can be retrieved from the increase or decrease in the bond orders observed in the FTIR spectrum of test and control.

In our study, the shift in corresponding peaks was observed in the broad stretch between the wavelength of 3,000 cm^{-1} – 3,500 cm^{-1} during zinc(II) adsorption, which suggests the presence of a large number of hydroxyl groups or water molecules. The range is also implicated for the stretching vibration of N-H groups present in proteins and their conjugates in the bacterial biomass. Similarly, doublet peaks observed in the region around 2,900 cm^{-1} may define the C-H stretch representative of the backbone of many major organic compounds including proteins and carbohydrates. The existence of groups like phosphates ($P=O$ and P-O seen in the C-PO_3 moiety) and C(=O)–O– and C–N stretching vibration were also detected as moderate bands around 1,250 cm^{-1} and 1,080 cm^{-1}. According to Bremer & Geesey (1991), a broad stretch around 1,000–1,200 cm^{-1} is caused by carbohydrates (C-O-C, C-O). In particular, the peaks between 1,000 and 1,125 cm^{-1} determine the existence of uronic acid, and o-acetyl ester linkage bonds. Changes in frequencies of the peaks below 600 cm^{-1} are often attributed to the creation of metal-ligand bond order (Kazy *et al.* 2006).

These observations overlap for both the test and control samples. The absence of any visible characteristic peaks in the spectrum points out the lack of chemical reaction of the metal ion with metal binding sites, if any, at the cell surface. Rather, it reveals the possibility of physisorption (or physical adsorption) as the main means of biosorption by *M. morganii* ACZ05.

The carbonyl, amine, phosphonate, sulfonate, and hydroxyl moieties are the most important groups accountable for the adherence of metal ions on bacterial cell walls. *M. morganii* is a Gram-negative bacterium with a cell wall that contains a thin peptidoglycan layer with 20% periplasmic space, and lipopolysaccharides along with specialized transporter proteins inside and outside the lipid membranes (Kumar 2018). Similarly, bacteria in the test samples are presumed to have secreted extracellular polymeric substances as a response to the stress caused by the presence of heavy metals in the media. The extracellular substances of microbes are also an intricate mixture of biopolymers containing polysaccharides, and surface polypeptides, uronic acids, and humic substances. These carry similar functional groups similar to that of the Gram-negative cell membrane. Similarities between functional groups of the cell membrane and EPS could also have resulted in the minor changes in the peak frequencies observed in the FTIR spectrum.

Both XRD and FTIR analysis observations strongly implicate the potential of physical adsorption as a mechanism of heavy metal resistance rather than other means of chemical sorption methods; that is, ion exchange, chelation, complexation. The absence of any chemical alterations to the cell membrane prompts the study of cell surface morphology to determine the extent of localized attachment of heavy metal ions to the surface. The surface morphology of the bacterial biomass was intensively investigated in the present work using AFM and SEM-EDX.

SEM has been quite frequently used correlatively with EDX in biosorption investigations. It helps in the analytical determination of the changes in cellular morphology, size, and volume (bacterial or otherwise), along with an elemental characterization of the cellular surface area. The changes in surface morphology were observed in the biomass of *M. morganii* strain ACZ05 before and after exposure of Zn^{2+} ions. Metal-less control showed distinct cell morphology as rod-shaped bacterial cells, with marked boundaries between them. Whereas, the bacterial cells exposed to metal exhibited various degrees of wrinkling and the loss of distinct peripheries between each cell. The formation of connected cell boundaries could be ascribed to the larger surface area provided by the bacteria for better and faster biosorption (Jin *et al.* 2017). Similarly,

Downloaded from http://iwaponline.com/wst/article-pdf/85/4/970/1016325/wst085040970.pdf
by guest

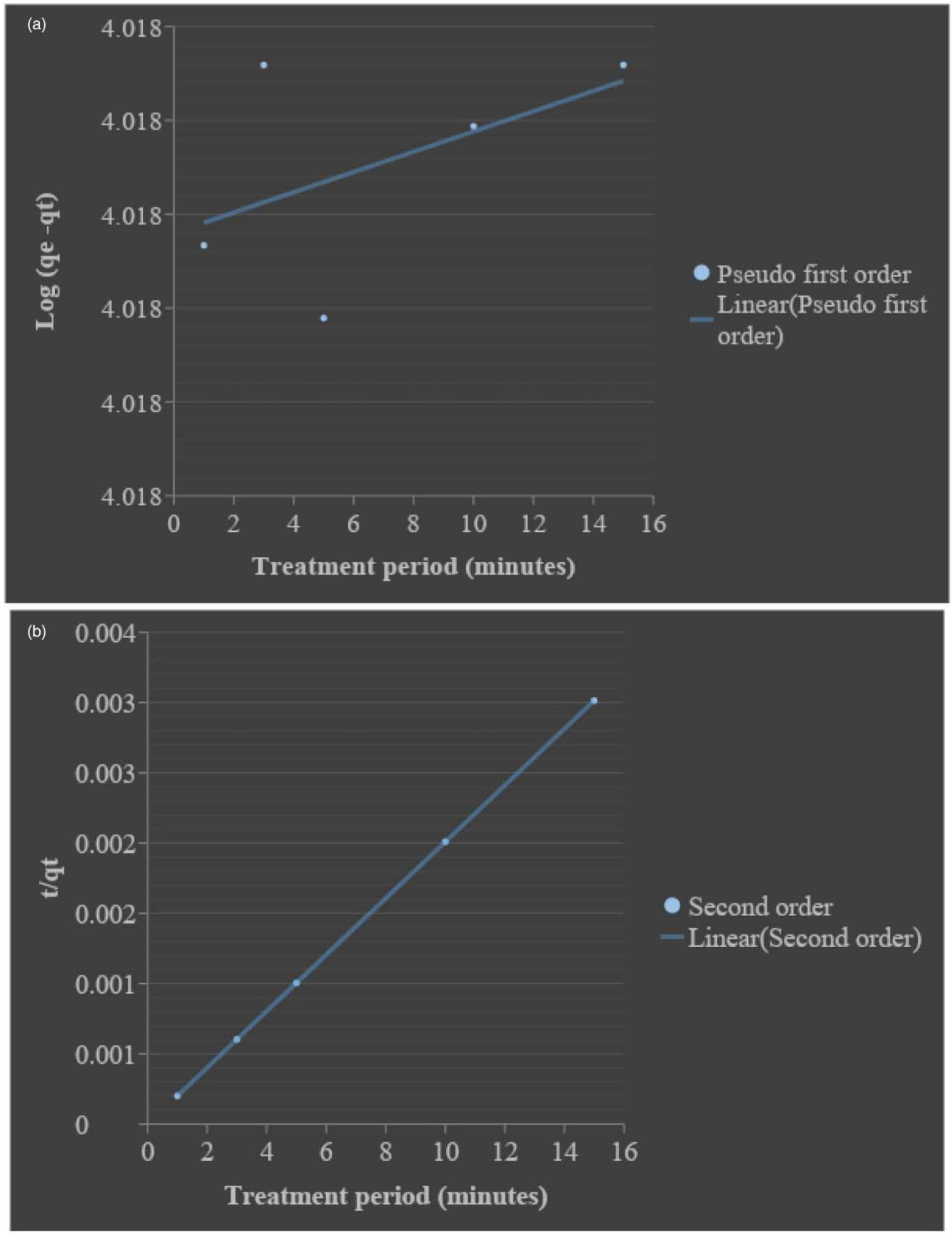

Figure 5 | Kinetics of adsorption of zinc by *M. morganii* ACZ05 for 500 mg/L of metal and 10 mg/100 mL of biomass concentration. (a) Pseudo-first order (b) Pseudo-second order.

Downloaded from http://iwaponline.com/wst/article-pdf/85/4/970/1016325/wst085040970.pdf
by guest

shrinkage and wrinkling of bacterial cells along with the development of the rough surface area is implemented to prevent heavy metal toxicity. Studies reported that bacteria grow in size up to a threshold concentration of heavy metals, while excess metal loading causes cell shrinkage and wrinkling. It is argued that live, metabolically active cells have a growth rate that is proportional to their surface area. Stress-induced morphological changes such as decreasing cell surface area available for heavy metal adsorption could be undertaken to increase metabolic activity and survival rate of the bacteria (Naik *et al.* 2012).

Another proposition which follows heavy metal resistance mechanisms in bacteria is the secretion of extracellular polymeric substances (EPS). Metaphorically, biofilms are called 'the city of microbes', and EPS is 'the house of biofilm cells' (Watnick & Kolter 2000; Flemming *et al.* 2007). EPS affects the bacterial microenvironment by changes in factors such as porosity, density, water content, charge, sorption properties, hydrophobicity, and mechanical stability (Flemming & Wingender 2003). In the present investigation, one of the stark changes between the control and test samples is the amorphous nature of the test sample. XRD and FTIR analysis carry testimony to the same. The metal-loaded bacterial biomass shows vigorous cell-to-cell adhesion and aggregation. It is visible that the number of bacterial cells observed in a unit area has also increased substantially from control to test. Formation of biofilm results in the multiplication of cells inside the microenvironment, leading to water retention, and an increase in adsorption properties. The EPS form a thick matrix inside which metal ions are often sequestered. The dark porous gaps observed in aggregated cell matrices seen in test bacterial biomass are inferred as water channels usually seen in biofilms. The absence of the structures in control is a conclusive indication of the formation of biofilm and secretion of EPS (Asahi *et al.* 2015).

Moreover, the SEM analysis of metal exposed bacterial biomass showed characteristic bright contrasted sections and new, glossy large particles on the cell surface in comparison to unexposed bacterial biomass. From literature, it is often inferred that localized cation deposition as a granular layer in a Gram-negative cell's envelope is usually attributed to the anionic nature of phosphoryl and carboxyl groups present in the cell's envelope. Previously, the presence of such relevant functional groups has been identified in both the test and control samples through FTIR. It follows through for Zn^{2+} ions, which are hard and bivalent cations (Sar *et al.* 2001).

In correlation with the results of SEM analysis, the very presence of a specific elemental peak of Zn(II) in the metal-loaded bacterial biomass and vice versa, fetches a conclusive identification of the physical adsorption of Zn^{2+} ions by this bacterial strain. Furthermore, changes in the elemental ratio of others are suggestive of different mechanisms behind the biosorption. EDX results also suggest peripheral localization of Zn^{2+} ions around the cell wall region, but rather due to ion exchange than sorption to available free sites. Similarly, an increase in the wt % of sulfur from 0.18 to 0.44 is also telling evidence of the adsorption of the $ZnSO_4$ complexes on the bacterial biomass.

The outcome of the EDX analysis also exposes the rise in the concentration of Mg, P, and Cl ions and cellular release of several new ions such as K, and Ca. Particularly, from these results it can be observed that the wt % of Na has completely disappeared from the cellular biomass from 0.13, while K has newly appeared at 0.22. Concerning metal homeostasis, this is typical of the Na^+/K^+/ATPase efflux pump. This particular phenomenon is usually ascribed to bacterial cells attempting to maintain metal ion homeostasis. Literature gives several instances where bacteria develop heavy metal resistance by adopting a variety of homeostatic functions and possessing different mechanisms for the transport of metal ions. So far, more than 100 P-type ATPases that act as metal transporter proteins have been discovered in bacteria as well as in other organisms (Agranoff & Krishna 1998). The binding of an extracellular counter-ion induces metabolism-coupled attachment and blocking of one or more intracellular cations. Among other strategies to reduce toxicity from metal ions, bacteria are also known to possess transmembrane transport proteins (metal ion/proton antiporters) in which proton gradients are utilized to transport metal ions with the expenditure of energy (Agranoff & Krishna 1998).

Yet another distinct feature is the considerable decrease in weight % of aluminum and silica ions from the cellular biomass. Previous studies suggest the exchange of zinc ions in the respective reactive sites in the metalloproteins found in the cell envelope and plasma membrane. The occurrence of the release of new metal ions through metal transporter proteins in the cell membrane can be inferred from the distinct peaks of aluminum and silica (Hase & Finkelstein 1993).

The scrutiny of AFM results is consistent with the findings of the SEM analysis. The control cells that have not been exposed to Zn^{2+} ions are found as elongated large in comparison to the metal-exposed cells. The metal-loaded biomass appeared much smaller in size as well as exhibiting aggregation into clusters. This is in relative correlation to SEM images, which showed the lack of distinct boundaries between individual cells. This supports earlier findings of cell shrinkage and wrinkling of bacterial biomass in response to excess metal loading than can be accommodated on the cell surface as well as intracellular homogenous distribution inside the cell periphery (Jin *et al.* 2017). As perceived from the topography scan of

Downloaded from http://iwaponline.com/wst/article-pdf/85/4/970/1016325/wst085040970.pdf
by guest

the AFM micrograph, the mean depth of the cell was found to reduce by almost fifty percent from control to test sample. It implies the consequent reduction in cell volume after metal ion adsorption. Moreover, the number of bacterial cells in the unit area was observed to have increased, which could indirectly be related to cell aggregation that occurs during biofilm production.

Previous studies argue the presence of surface proteins in the S-layer of the bacterium or the functional groups with strong metal binding tendencies found in the lipopolysaccharides of the Gram-negative bacterial strains, which promote the formation of sequestration of the metal ions into the biofilm matrix via extracellular polymeric substances (EPS) beyond threshold concentration. Similarly, the absence of integrity and consequent ambiguity in the cell boundaries, and aggregation of bacterial biomass to maintain the reduction in individual cell surface area suggest that these morphological changes have been adapted for stress-induced survival mechanisms (Kazy *et al.* 2008).

The results concur with each other in the possibility of reduction in cell size and surface area as a metabolism-dependent survival mechanism following physical adsorption, ATPase-mediated transporting of hard cations, and EPS secretion. Similar findings were reported in a study using *Pseudomonas* and spores of *Bacillus* species SG-1 strain to remove copper from wastewater (Gavrilescu 2004).

The Langmuir, Freundlich and Sips isotherms are not a good fit for the experimental data on all four days. The only exception to the above data is day one for the Freundlich isotherm, wherein the R^2 value is 0.99, making it a very good fit. However, the correlation coefficient for Langmuir isotherm models was extreme at day one of adsorption (0.33) and the values were far below the threshold of $R^2 > 0.9$. The adsorption capacity constant (Q_{max}) and affinity constant (b) for Langmuir were largely intermittent values, and thereby considered negotiable.

The Freundlich constants K_f and n exhibited an upward curve from day one onwards, reaching maximum on day four. Meanwhile, the Freundlich constants K_f and n describing the volume and strength of adsorption were quantifiable values on day one ($4.44E17 \times 10^{-8}$, 0.12). Due to the low fit of the experimental data derived up to a treatment period of four days, the treatment period is recommended to be reduced to minutes. The low R^2 values could also be attributed to an insufficient range of concentration of metals available to the cell surface, or the possibility of saturation until equilibrium long before measurement of data.

Biosorption of zinc (II) by dead *Pseudomonas putida* biomass showed a perfect fit to the Langmuir isotherm model. In this model, metal ions maintained by the biomass growth up to a constant value, due to the liberal reduction of the free attaching sites on the cell wall. But the Freundlich model did not fit the data with the exclusion of the first data points and hence this model is only appropriate at low zinc (II) metal concentrations (Pardo *et al.* 2003). Elimination of zinc (II) by papaya wood was reported and the initial concentrations of zinc (II) varied from (5–500 mg/L) for the fixed mass of papaya wood (5 g/L) for the sorbate–sorbent interaction time of 60 min. The biosorption of zinc (II) data fit the Langmuir isotherm model with correlation coefficient of R^2 value 0.99 than the Freundlich adsorption isotherm model (Saeed *et al.* 2005).

In the bioremoval abilities of Zn (I1) ions in aqueous solution using *Aspergillus niger,* the utmost uptake abilities were 23.70 mg/g of biomass with preliminary metal ion concentrations of 150 mg/L for Zn (I1) ions. The biosorption of zinc ions perfectly fits the Langmuir model (Liu *et al.* 2006). For the biosorption of zinc (II) in an aqueous solution by coir, the biosorption isotherm data of the Langmuir model was not appropriate for the sorption of Zn (II) ions. But sorption of zinc (II) data fit the Freundlich isotherm model with correlation coefficient of R^2 value, 0.99 (Conrad & Hansen 2007).

Joo *et al.* (2010) stated that the removal of Zn (II) by lyophilized cells of *Bacillus cereus* AUMC B52 and *Pseudomonas aeruginosa* ASU 6a at a preliminary concentration of 0–200 mg/L and 30 min interaction time. The sorption data fitted properly with the Langmuir and Freundlich adsorption isotherm equations in the investigated range of metal concentration. The results showed that the biosorption of Zn (II) by *P. aeruginosa* ASU 6a was greater than using *B. cereus* AUMC B52. The b values of freeze-dried cells of *B. cereus* AUMC B52 and *P. aeruginosa* ASU 6a for Zn (II) were 0.048 and 0.035 mg/L, respectively. Chubar *et al.* (2008) stated that the maximum biosorption ability by *Shewanella putrefaciens* was 34 mg/g.

The study of the kinetics of metal uptake in the biosorption process is necessary to understand the rate of the process, the optimum conditions required in a batch process reactor, as well as the nature of the adsorption process. Among various models, Lagregen's pseudo-first and Blanchard's second-order equations are employed widely to determine the operating parameters of the biosorption process. Even though the current understanding of the kinetics of the biosorption process is much less, the differences between the correlation coefficient of both kinetics models are utilized to explain the experimental data.

On a similar note, rate kinetics was calculated at particular time intervals of biosorption of zinc onto *M. morganii* ACZ05 biomass and data found were plotted against time to determine a desirable kinetic model. The R^2 values as a coefficient of determination specified that the R^2 values for pseudo-second-order were greater than that of the pseudo-first-order.

Downloaded from http://iwaponline.com/wst/article-pdf/85/4/970/1016325/wst085040970.pdf
by guest

The layout of a reactor, reaction parameters, and sorption kinetics are necessary to apply *in situ* and *ex-situ* (Azizian 2004). The biosorption mechanism, rate of reaction, and its pathway are important in effluent treatment (Ho & McKay 1999a, 1999b). At the biosorbent-metal ion interface, the kinetics of the reaction hinges upon metal intake and duration of exposure to bacterial biomass (Ho *et al.* 2000). Meanwhile, biosorption independent of the cell's metabolism, as is predicted to be a rapid method. Bacterial biomass and metal ion equilibrium are achieved in batch reactor conditions in two stages: first 30 mins to one hour followed by the slow forward reaction within 120–180 minutes (Celaya *et al.* 2000; Choi & Yun 2004; Lu *et al.* 2006).

The rate kinetics was calculated at particular time intervals of biosorption of zinc onto *M. morganii* ACZ05 biomass and data was found and plotted against time to determine a desirable kinetic model. The R^2 values as a coefficient of determination specified that the R^2 values for pseudo-second-order were greater than the pseudo-first-order. Pseudo-first-order kinetics assume a bimolecular reaction between the adsorbent and the adsorbate, whereas a biosorption reaction between the cell membrane, efflux pumps and exopolysaccharides present in the biofilm can be hardly considered as a bimolecular interaction between a single type of binding site and metal ion. A pseudo first order reaction is often hard to characterise such a highly heterogeneous reaction between the bacterial biomass and the metal ion.

5. CONCLUSION

Characterization of the mechanism of biosorption reveals the possibility of biofilm production by *Morganella morganii* due to zinc (II) exposure. Applying linear models of isotherm equations was found to be insufficient to describe the interaction of metal ions on the heterogeneous cell surface. The highly significant fit of pseudo-second-order for biosorption experimental data of Zn (II) ions by *M. morganii* ACZ05 suggests the involvement of cellular mechanisms for the activity of binding sites of metal ions and other chemical sorption processes. Various mechanisms such as metabolism-independent physical adsorption, and extracellular polysaccharide production, and efflux transport of metal ions through pumps such as ATPases, could be adapted by bacteria to maintain electro-neutrality and osmotic balance, which requires further study.

ACKNOWLEDGEMENTS

The authors are grateful to the University Grants Commission, New Delhi for the financial assistance provided for the Major Research Project (F.no: 40-368/2011(SR)). They also extend their thanks to the administrators of The American College, Madurai, for the infrastructure and encouragement extended for the successful conduct of the project.

DATA AVAILABILITY STATEMENT

All relevant data are included in the paper or its Supplementary Information.

REFERENCES

Agranoff, D. D. & Krishna, S. 1998 Metal ion homeostasis and intracellular parasitism. *Mol. Microbiol.* **28**, 403–412.

Ahalya, N., Ramachandra, T. V. & Kanamadi, R. D. 2003 Biosorption of heavy metals. *Res. J. Chem. Environ.* **7**, 71–79.

Ahluwalia, S. S. & Goyal, D. 2007 Microbial and plant derived biomass for removal of heavy metals from wastewater. *Bioresour. Technol.* **98**, 2243–2257.

Asahi, Y., Miura, J., Tsuda, T., Kuwabata, S., Tsunashima, K., Noiri, Y. & Hayashi, M. 2015 Simple observation of *Streptococcus mutans* biofilm by scanning electron microscopy using ionic liquids. *AMB Express* **5**, 6.

Azizian, S. 2004 Kinetic models of sorption: a theoretical analysis. *J. Colloid Interface Sci.* **276**, 47–52.

Bremer, P. J. & Geesey, G. G. 1991 An evaluation of biofilm development utilizing non-destructive attenuated total reflectance Fourier transform infrared spectroscopy. *Biofouling* **3**, 89–100.

Celaya, R. J., Noriega, J. A., Yeomans, J. H., Ortega, L. J. & Ruiz-Manriquez, A. 2000 Biosorption of Zn (II) by *Thiobacillus ferrooxidans*. *Bioprocess Eng.* **22**, 539–542.

Çeribasi, I. H. & Yetis, U. 2001 Biosorption of Ni (II) and Pb (II) by *Phanerochaetechrysosporium* from a binary metal system–kinetics. *Water SA* **27**, 15–20.

Choi, S. B. & Yun, Y. S. 2004 Lead biosorption by waste biomass of *Corynebacterium glutamicum* generated from lysine fermentation process. *Biotechnol. Lett.* **26**, 331–336.

Chubar, N., Behrends, T. & Van Cappellen, P. 2008 Biosorption of metals (Cu^{2+}, Zn^{2+}) and anions (F^{-}, $H2PO^{4-}$) by viable and autoclaved cells of the Gram-negative bacterium *Shewanella putrefaciens*. *Colloids Surf. B* **65**, 126–133.

Conrad, K. & Hansen, H. C. B. 2007 Sorption of zinc and lead on coir. *Bioresour. Technol.* **98**, 89–97.

Downloaded from http://iwaponline.com/wst/article-pdf/85/4/970/1016325/wst085040970.pdf
by guest

Deokar, A. R., Lin, L. Y., Chang, C. C. & Ling, Y. C. 2013 Single-walled carbon nanotube coated antibacterial paper: preparation and mechanistic study. *J. Mater. Chem B* **1**, 2639–2646.

Derco, J. & Vrana, B. 2018 Introductory chapter: biosorption. *Biosorption Intech Open* **1**, 1–19.

Devika, M. V., Thatheyus, A. J. & Ramya, D. 2014 Bioremoval of nickel using *Pseudomonas aeruginosa*. *Annu. Res. Rev. Biol.* **4**, 538–546.

Flemming, H. C. & Wingender, J. 2003 Extracellular polymeric substances (EPS): structural, ecological and technical aspects. In: Bitton, G. (ed) *Encyclopedia of Environmental Microbiology*. John Wiley & Sons, New York, NY.

Flemming, H. C., Neu, T. R. & Wozniak, D. J. 2007 The EPS matrix: the 'house of biofilm cells'. *J. Bacteriol.* **189**, 7945–7947.

Fomina, M. & Gadd, G. M. 2014 Biosorption: current perspectives on concept, definition and application. *Bioresour. Technol.* **160**, 3–14.

Gabr, R. M., Hassan, S. H. A. & Shoreit, A. A. M. 2008 Biosorption of lead and nickel by living and non-living cells of *Pseudomonas aeruginosa* ASU 6a. *Int. Biodeterior. Biodegr.* **62**, 195–203.

Gadd, G. M. 2009 Biosorption: critical review of scientific rationale, environmental importance and significance for pollution treatment. *J. Chem. Technol. Biotechnol.* **84**, 13–28.

Gavrilescu, M. 2004 Removal of heavy metals from the environment by biosorption. *Eng. Life Sci.* **4**, 219–232.

Hase, C. C. & Finkelstein, R. A. 1993 Bacterial extracellular zinc-containing metalloproteases. *Microbiol. Mol. Biol. Rev.* **57**, 823–837.

Ho, Y. S. & McKay, G. 1999a Comparative sorption kinetic studies of dye and aromatic compounds onto fly ash. *J. Environ. Sci. Health Part A* **34**, 1179–1204.

Ho, Y. S. & McKay, G. 1999b Pseudo-second order model for sorption processes. *Process Biochem.* **34**, 451–465.

Ho, Y. S., McKay, G., Wase, D. A. J. & Forster, C. F. 2000 Study of the sorption of divalent metal ions on to peat. *Adsorpt. Sci. Technol.* **18**, 639–650.

Horsfall Jnr, M. & Spiff, A. I. 2005 Effects of temperature on the sorption of Pb^{2+} and Cd^{2+} from aqueous solution by Caladium bicolor (Wild Cocoyam) biomass. *Electron. J. Biotechnol* **8** (2), 43–50.

Huang, W. & Liu, Z. M. 2013 Biosorption of Cd (II)/Pb (II) from aqueous solution by biosurfactant-producing bacteria: isotherm kinetic characteristic and mechanism studies. *Colloids Surf. B* **105**, 113–119.

Hussein, H., Ibrahim, S. F., Kandeel, K. & Moawad, H. 2004 Biosorption of heavy metals from waste water using Pseudomonas sp. *Electron J. Biotechnol* **7** (1), 30–37.

Jin, Y., Yu, S., Teng, C., Song, T., Dong, L., Liang, J. & Qu, J. 2017 Biosorption characteristic of Alcaligenes sp. BAPb. 1 for removal of lead (II) from aqueous solution. *3 Biotech.* **7**, 123.

Joo, J. H., Hassan, S. H. & Oh, S. E. 2010 Comparative study of biosorption of Zn^{2+} by *Pseudomonas aeruginosa* and *Bacillus cereus*. *Int. Biodeter. Biodegr.* **64**, 734–741.

Kazy, S. K., Das, S. K. & Sar, P. 2006 Lanthanum biosorption by a *Pseudomonas* sp.: equilibrium studies and chemical characterization. *J. Ind. Microbiol. Biotechnol.* **33**, 773–783.

Kazy, S. K., Sar, P. & D'Souza, S. F. 2008 Studies on uranium removal by the extracellular polysaccharide of a *Pseudomonas aeruginosa* strain. *Bioremediat. J.* **12**, 47–57.

Kazy, S. K., D'Souza, S. F. & Sar, P. 2009 Uranium and thorium sequestration by a *Pseudomonas* sp.: mechanism and chemical characterization. *J. Hazard. Mater.* **163**, 65–72.

Kotrba, P. 2011 Microbial biosorption of metals – general introduction. In: Kotrba, P., Macek, T. & Mackova, M. (eds) *Microbial Biosorption of Metals*. Springer, Dordrecht, the Netherlands, pp. 1–6.

Kumar, A., Bisht, B. S. & Joshi, V. D. 2010 Biosorption of heavy metals by four acclimated microbial species, Bacillus spp., Pseudomonas spp., Staphylococcus spp. *and Aspergillus niger. J. Biol. Environ. Sci.* **4** (12), 97–108.

Kumar, V. 2018 Mechanism of microbial heavy metal accumulation from a polluted environment and bioremediation. In: *Microbial Cell Factories*. CRC Press, Boca Raton, FL, pp. 149–174.

Kumar, P., Maurya, A., Garg, S., Yadav, A., Mishra, V. & Sharma, R. S. 2020 Dead biomass of *Morganella morganii* acts as an efficient adsorbent to remove Pb (II) from aqueous solution in different aeration–agitation and pH conditions. *SN Appl. Sci.* **2** (7), 1–10.

Liu, Y. G., Ting, F. A. N., Zeng, G. M., Xin, L. I., Qing, T., Fei, Y. E. & Huang, Y. E. 2006 Removal of cadmium and zinc ions from aqueous solution by living Aspergillus niger. *Trans. Nonferrous Met. Soc. China* **16** (3), 681–686.

Lu, W. B., Shi, J. J., Wang, C. H. & Chang, J. S. 2006 Biosorption of lead, copper and cadmium by an indigenous isolate *Enterobacter* sp. J1 possessing high heavy-metal resistance. *J. Hazard. Mater.* **134**, 80–86.

Martins, M., Faleiro, M. L., Chaves, S., Tenreiro, R., Santos, E. & Costa, M. C. 2010 Anaerobic bio-removal of uranium (VI) and chromium (VI): comparison of microbial community structure. *J. Hazard. Mater.* **176**, 1065–1072.

Naik, U. C., Srivastava, S. & Thakur, I. S. 2012 Isolation and characterization of *Bacillus cereus* IST105 from electroplating effluent for detoxification of hexavalent chromium. *Environ. Sci. Pollut. Res.* **19**, 3005–3014.

Oh, S. E., Hassan, S. H. & Joo, J. H. 2009 Biosorption of heavy metals by lyophilized cells of *Pseudomonas stutzeri*. *World J. Microb. Biotechnol.* **25**, 1771–1778.

Pagnanelli, F., Petrangeli Papini, M., Toro, L., Trifoni, M. & Veglio, F. 2000 Biosorption of metal ions on *Arthrobacter* sp.: biomass characterization and biosorption modeling. *Environ. Sci. Technol.* **34**, 2773–2778.

Pardo, R., Herguedas, M., Barrado, E. & Vega, M. 2003 Biosorption of cadmium, copper, lead and zinc by inactive biomass of *Pseudomonas putida*. *Anal. Bioanal. Chem.* **376**, 26–32.

Park, D., Yun, Y. S. & Park, J. M. 2010 The past, present, and future trends of biosorption. *Biotechnol. Bioprocess Eng.* **15**, 86–102.

Downloaded from http://iwaponline.com/wst/article-pdf/85/4/970/1016325/wst085040970.pdf
by guest

Princy, S., Sathish, S. S., Cibichakravarthy, B. & Prabagaran, S. R. 2020 Hexavalent chromium reduction by *Morganella morganii* (1Ab1) isolated from tannery effluent contaminated sites of Tamil Nadu, India. *Biocatal. Agric. Biotechnol.* **23**, 101469.

Saeed, A., Akhter, M. W. & Iqbal, M. 2005 Removal and recovery of heavy metals from aqueous solution using papaya wood as a new biosorbent. *Sep. Purif. Technol.* **45**, 25–31.

Sar, P., Kazy, S. K. & Singh, S. P. 2001 Intracellular nickel accumulation by *Pseudomonas aeruginosa* and its chemical nature. *Lett. Appl. Microbiol.* **32**, 257–261.

Shimazu, A., Miyazaki, T. & Ikeda, K. 2000 Interpretation of d-spacing determined by wide angle X-ray scattering in 6FDA-based polyimide by molecular modeling. *J. Membr. Sci.* **166**, 113–118.

Sips, R. 1948 Combined form of Langmuir and Freundlich equations. *J. Chem. Phys.* **16**, 490–495.

Srivastava, S. & Thakur, I. S. 2007 Evaluation of biosorption potency of *Acinetobacter* sp. for removal of hexavalent chromium from tannery effluent. *Biodegradation* **18**, 637–646.

Teitzel, G. M. & Parsek, M. R. 2003 Heavy metal resistance of biofilm and planktonic Pseudomonas aeruginosa. *Applied and environmental microbiology* **69** (4), 2313–2320.

Wang, J. & Chen, C. 2009 Biosorbents for heavy metals removal and their future. *Biotechnol. Adv.* **27** (2), 195–226.

Watnick, P. & Kolter, R. 2000 Biofilm, city of microbes. *J. Bacteriol* **182** (10), 2675–2679.

First received 10 August 2021; accepted in revised form 14 January 2022. Available online 29 January 2022

Downloaded from http://iwaponline.com/wst/article-pdf/85/4/970/1016325/wst085040970.pdf
by guest